Novel control strategy for the global model of wind turbine

Yattou El Fadili, Youssef Berrada, Ismail Boumhidi
Computer Science, Signal, Automation, and Cognitivism Laboratory, Department of Physics, Faculty of Sciences, Sidi Mohamed Ben Abdellah University, Fez, Morocco

Article Info	ABSTRACT
	This paper presents a new nonlinear control for the overall model of a three-blade horizontal axis variable speed wind turbine (VSWT) including mechanical and electrical parts, with the aim of improving its performance and making it more profitable. The proposed control is an extension of the classical sliding mode control (SMC) by converting its sliding surface into a sliding sector. The classical SMC approach is widely used for nonlinear systems due to its stability against parameter variation, it is robustness against modeling uncertainties, its good results against external disturbances, and its ease of implementation in real time. Unfortunately, the SMC has a major drawback related to the chattering phenomenon. This phenomenon is due to the utility of a higher switching gain in the case of large uncertainties, it causes high-frequency oscillations once the sliding regime is reached, and it can cause a loss of accuracy by influencing the input control variables. This is the reason that aims to develop a new control law to eliminate the chattering and to guarantee stability, which is demonstrated by the Lyapunov theory. The effectiveness of the developed control is compared with the SMC and is illustrated by numerical simulations using MATLAB toolboxes. *This is an open access article under the CC BY-SA license.*

Corresponding Author:

Yattou El Fadili
Computer Science, Signal, Automation, and Cognitivism Laboratory, Physics Department, Faculty of
Sciences Dhar El Mahraz, Sidi Mohamed Ben Abdellah University
B. P. 1796 Fez-Atlas, 30003, Fez, Morocco
Email: yattou.elfadili@usmba.ac.ma

1. INTRODUCTION

In recent decades, the most widely used source of renewable energy has been the wind energy conversion system [1]–[5]. The interest in the wind turbine (WT) goes back to it is benefits as a sustainable, renewable, clean energy source, it is simplicity of installation, and its small surface occupation. The general idea of wind power is to harness the kinetic energy of wind by transforming it into electrical energy. The modern WT as depicted in Figure 1 is the horizontal axis variable speed wind turbine (VSWT) with three-blade [6], [7]. The VSWT contains an aeroturbine coupled to a doubly-fed induction generator (DFIG) as depicted in Figure 1(a) [8], [9]. The WT has a highly non-linear mathematical model as depicted in Figure 1(b) and its dynamics change rapidly with fluctuations in wind speed [10].

The wind is an uncontrollable parameter that causes parametric variations in the structure of the WT, cannot stabilize it, and affects its economic viability. Therefore, researchers and engineers are thinking of developing more effective control laws to increase the WT's efficiency and improve the performance of the WT that operate under turbulent, random, and unpredictable wind speed. In the literature, some works have been done on the control of the mechanical subsystem without taking into consideration the control of the electrical part [11], while other research has been done on the control of the electrical part without taking into account the mechanical part [12]–[15]. This is the main contribution that motivates us in this paper to

perform work concerning the control of the global WT while taking into account both studies of the mechanical and electrical parts. Among the existing control methods in the literature, the linearization technique is a common strategy that aims to surmount the problem of nonlinearity. However, controllers designed mainly using the technique of WT linearization around their operating points [16] lead to reduced system performance [17]. Other non-linear techniques for the control of WT of which the most used is the sliding mode control (SMC) law. The SMC law is a powerful nonlinear control approach that has been deeply studied and applied in different practical applications [18], [19] among them the WT systems [20]–[22]. Unfortunately, the SMC has a major drawback named the chattering phenomenon that results from the discontinuity of the control law and the real dynamic behavior of the WT. The chattering problem is undesirable because causes rapid control signal variations which lead to high-frequency oscillations that damage the WT [23].
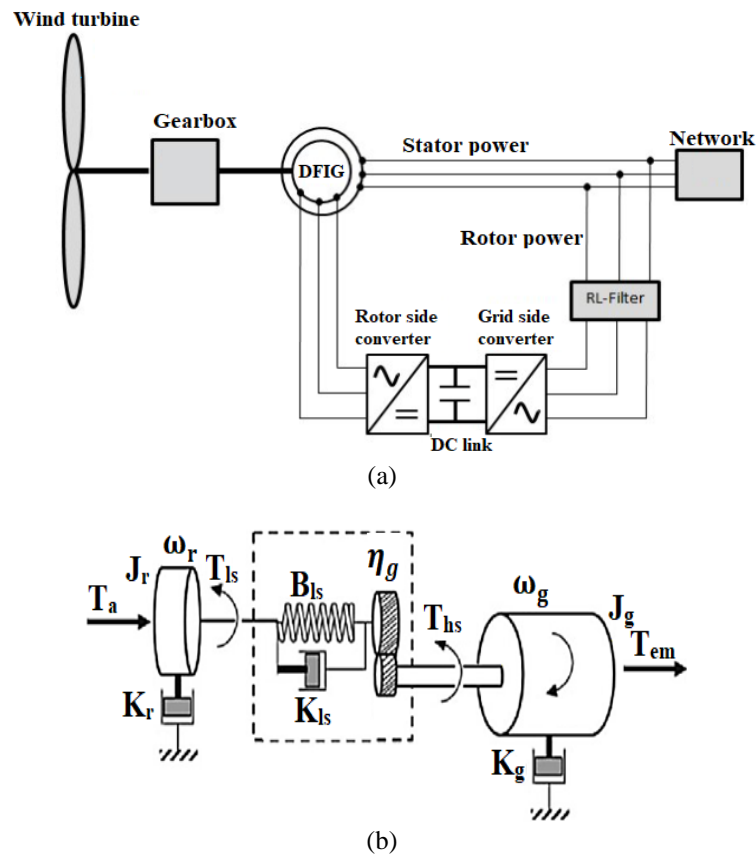

(a)

(b)

Figure 1. Complete wind turbine model (a) DFIG electrical model, and (b) two-mass mechanical model

The strong contribution of this article is to tackle the major drawback of SMC (i.e., the chatter phenomenon). This paper presents a developed law for controlling the whole model of WT including both mechanical and electrical parts. The proposed new technique of control is extensively studied and analyzed which is an extension of the classical SMC law by transforming its sliding surface into a sliding sector as in [24]. The developed control law is called the sliding sector control (SSC). The good performances of the developed control strategy are demonstrated by the simulation results using MATLAB toolboxes in terms of precise tracking of the rotor speed and its reference signal, maximum extracting of wind energy whatever the climatic change, reducing aerodynamic loads in order to increase the lifespan of WT, achieving stability and robustness against modeling uncertainties and external disturbances represented by rapid wind speed variations, eliminating the chattering phenomenon, and using a high value of switching gain.

The main sections are as follows: section 2 gives the mathematical models of the mechanical part, the electrical part, and the whole WT followed by the proposed control for the entire WT. In section 3, the WT's performances are depicted and compared to classical SMC. The conclusion is given in section 4 which summarizes the highlights of this present paper.

2. MODEL OF WIND TURBINE SYSTEM

The three-blade horizontal axis VSWT is divided into two subsystems which are the mechanical and the electrical subsystems which are connected together. To model this type of wind turbine, the models of the mechanical and the electrical subsystems are necessary. In the context of controlling the entire wind turbine, some notations are adopted throughout this paper, presented in Table 1 to help the readers and researchers, are listed to refer to the specific coefficients easily and understand the proposed design control.

Table 1. WT notations of the different coefficients

Coefficient	Notation
Gearbox ratio	η_g
Wind speed	v
Aerodynamic torque	T_a
Rotor speed	ω_r
Rotor inertia	J_r
Rotor external friction	K_r
Low-speed shaft torque	T_{ls}
Slow shaft torsion	B_{ls}
Slow shaft friction	K_{ls}
Fast-speed shaft torque	T_{hs}
Generator speed	ω_g
Generator inertia	J_g
Generator external friction	K_g
Electromagnetic torque	T_{em}
Rotor d-axis current/q-axis current	I_{rd}/I_{rq}
Stator d-axis current/q-axis current	I_{sd}/I_{sq}
Rotor angular speed	ϖ_r
Synchronous angular speed	ϖ_s
Switching gain	α
Pole number	P
Stator active power/reactive power	P_s/Q_s
Scattering coefficient	σ
Pitch angle	β
Stator d-axis flux/q-axis flux	ϕ_{sd}/ϕ_{sq}
Rotor q-axis flux/d-axis flux	ϕ_{rq}/ϕ_{rd}
Rotor inductance	L_r
Stator inductance	L_s
Rotor resistance	R_r
Stator resistance	R_s
Aerodynamic power	P_a
Stator d-axis voltage	V_{sd}
Stator q-axis voltage	V_{sq}
Mutual inductance	L_m
Rotor d-axis voltage	V_{rd}
Rotor q-axis voltage	V_{rq}

2.1. Mechanical part model

The mechanical part of WT is depicted in Figure 1(b). To model the mechanical part, the two-mass model is used. The modeling of the mechanical part is given in (1) [24].

$$
\begin{cases}
\dot{\omega}_r = -\frac{K_r}{J_r} \times \omega_r - \frac{1}{J_r} \times T_{ls} + \frac{1}{J_r} \times T_a \\
\dot{\omega}_g = -\frac{K_g}{J_g} \times \omega_g + \frac{1}{J_g \times \eta_g} \times T_{ls} - \frac{1}{J_g} \times T_{em} \\
\dot{T}_{ls} = \left(B_{ls} - \frac{K_{ls} \times K_r}{J_r}\right) \times \omega_r + \left(\frac{K_{ls} \times K_g}{J_g \times \eta_g} - \frac{B_{ls}}{\eta_g}\right) \times \omega_g - \frac{k_{ls} \times (J_r + J_g \times \eta_g^2)}{\eta_g^2 \times J_g \times J_r} \times T_{ls} + \frac{k_{ls}}{J_r} \times T_a + \frac{k_{ls}}{J_g \times \eta_g} \times T_{em}
\end{cases} \tag{1}
$$

2.2. Electrical part model

The analysis of the electrical part of the modern WT goes back to analyzing the DFIG. The WT's DFIG is described by its stator which is linked to the network, and its rotor is coupled to the network through a power converter [25]. Figure 1(a) shows the overall WT design including the connection of the aeroturbine and the DFIG. To simplify this analysis, two simplifying assumptions are taken into account. The first is that the stator resistance is neglected. The second is that the q-axis of the Park's reference is aligned with the stator voltage. These hypotheses will lead to the equations as in (2) [26], [27].

$$
\begin{cases}
\phi_{sd} = \phi_s \\
\phi_{sq} = 0 \\
V_{sd} = 0 \\
V_{sq} = \varpi_s \phi_s \\
\phi_{rd} = \sigma L_r I_{rd} + \frac{L_m \phi_s}{L_s} \\
\phi_{rq} = \sigma L_r I_{rq} \\
V_{rd} = R_r I_{rd} + \sigma L_r \dot{I}_{rd} - \varpi_r \sigma L_r I_{rq} \\
V_{rq} = R_r I_{rq} + \sigma L_r \dot{I}_{rq} + \varpi_r \sigma L_r I_{rd} + \frac{\varpi_r L_m \phi_s}{L_s} \\
T_{em} = -\frac{pL_m \phi_s}{L_s} I_{rq} \\
P_s = -\frac{\varpi_s L_m \phi_s}{L_s} I_{rq} \\
Q_s = \frac{\varpi_s \phi_s^2}{L_s} - \frac{\varpi_s L_m \phi_s}{L_s} I_{rd}
\end{cases}
\tag{2}
$$

2.3. Overall model of wind turbine

The entire WT model is modeled as in (3). The whole WT model is obtained by combining the mechanical subsystem model using the two-mass model presented in subsection 2.1 and the electrical subsystem model given in subsection 2.2. The entire WT model is given by taking into account the system's input is the rotor q-axis voltage noted by u and the system's output is the rotor speed. The main used coefficients in (3) of the whole WT model are identified at the end of this subsection 2.3.

$$
\begin{pmatrix} \dot{\omega}_r \\ \dot{\omega}_g \\ \dot{T}_{ls} \\ \dot{T}_{em} \\ \dot{I}_{rq} \\ \dot{I}_{rd} \end{pmatrix} =
\begin{pmatrix}
a_{11} & a_{12} & a_{13} & a_{14} & a_{15} & a_{16} \\
a_{21} & a_{22} & a_{23} & a_{24} & a_{25} & a_{26} \\
a_{31} & a_{32} & a_{33} & a_{34} & a_{35} & a_{36} \\
a_{41} & a_{42} & a_{43} & a_{44} & a_{45} & a_{46} \\
a_{51} & a_{52} & a_{53} & a_{54} & a_{55} & a_{56} \\
a_{61} & a_{62} & a_{63} & a_{64} & a_{65} & a_{66}
\end{pmatrix} \times
\begin{pmatrix} \omega_r \\ \omega_g \\ T_{ls} \\ T_{em} \\ I_{rq} \\ I_{rd} \end{pmatrix} +
\begin{pmatrix} b_1 \\ b_2 \\ b_3 \\ b_4 \\ b_5 \\ b_6 \end{pmatrix} \times u(t) +
$$

$$
\begin{pmatrix}
c_{11} & c_{12} & c_{13} & c_{14} \\
c_{21} & c_{22} & c_{23} & c_{24} \\
c_{31} & c_{32} & c_{33} & c_{34} \\
c_{41} & c_{42} & c_{43} & c_{44} \\
c_{51} & c_{52} & c_{53} & c_{54} \\
c_{61} & c_{62} & c_{63} & c_{64}
\end{pmatrix} \times
\begin{pmatrix} T_a \\ V_{rd} \\ \phi_s \\ V_{rq} \end{pmatrix}
\tag{3}
$$

$a_{11} = -\frac{K_r}{J_r};$ $a_{12} = 0;$ $a_{13} = -\frac{1}{J_r};$ $a_{14} = 0;$ $a_{15} = 0;$ $a_{16} = 0;$

$a_{21} = 0;$ $a_{22} = -\frac{K_g}{J_g};$ $a_{23} = \frac{1}{J_g \eta_g};$ $a_{24} = -\frac{1}{J_g};$ $a_{25} = 0;$ $a_{26} = 0;$

$a_{31} = \frac{B_{ls}J_r - K_{ls}K_r}{J_r};$ $a_{32} = \frac{K_{ls}K_g - B_{ls}J_g}{J_g \eta_g};$ $a_{33} = -K_{ls}\frac{J_r + J_g \eta_g^2}{J_r J_g \eta_g^2};$ $a_{34} = \frac{K_{ls}}{\eta_g J_g};$ $a_{35} = 0;$ $a_{36} = 0;$

$a_{41} = 0;$ $a_{42} = 0;$ $a_{43} = 0;$ $a_{44} = 0;$ $a_{45} = \frac{pL_m \phi_s R_r}{\sigma L_r L_s};$ $a_{46} = \frac{pL_m \phi_s \varpi_r}{L_s};$

$a_{51} = 0;$ $a_{52} = 0;$ $a_{53} = 0;$ $a_{54} = 0;$ $a_{55} = -\frac{R_r}{\sigma L_r};$ $a_{56} = -\varpi_r;$

$a_{61} = 0;$ $a_{62} = 0;$ $a_{63} = 0;$ $a_{64} = 0;$ $a_{65} = \varpi_r;$ $a_{66} = -\frac{R_r}{\sigma L_r};$

$b_1 = 0;$ $b_2 = 0;$ $b_3 = 0;$ $b_4 = -\frac{pL_m \phi_s}{\sigma L_r L_s};$ $b_5 = 0;$ $b_6 = 0;$

$c_{11} = \frac{1}{J_r};$ $c_{21} = 0;$ $c_{31} = \frac{K_{ls}}{J_r};$ $c_{41} = 0;$ $c_{51} = 0;$ $c_{61} = 0;$

$c_{12} = 0;$ $c_{22} = 0;$ $c_{32} = 0;$ $c_{42} = 0;$ $c_{52} = 0;$ $c_{62} = \frac{1}{\sigma L_r};$

$c_{13} = 0;$ $c_{23} = 0;$ $c_{33} = 0;$ $c_{43} = \frac{p\varpi_r \phi_s L_m^2}{\sigma L_r L_s^2};$ $c_{53} = -\frac{\varpi_r L_m}{\sigma L_r L_s};$ $c_{63} = 0;$

$c_{14} = 0;$ $c_{24} = 0;$ $c_{34} = 0;$ $c_{44} = 0;$ $c_{54} = \frac{1}{\sigma L_r};$ $c_{64} = 0.$

2.4. Application of sliding sector control for wind turbines

The proposed novel control law that is called SSC. This novel law is developed based on the classical strategy of SMC by transforming its sliding surface into a sliding sector. The sliding sector consists of multiple sliding sub-surfaces [24]. The number of the sub-surfaces depends on the system's relative degree which is determined through the calculation of successive derivatives of the tracking error. The main objective of the SSC is to eliminate the chattering phenomenon that appears during the reaching phase. In this paper, the relative degree is three which means the utility of three sub-surfaces that define the boundaries of

the sliding sector which represents their center. The fundamental steps of SSC are selecting the sliding sector, constructing the control law, and establishing the existence conditions. To design of SSC controller for the whole WT model, the system's input is rotor q-axis voltage and the system's output is rotor speed. The controller should ensure the rotor speed follows its reference signal. The tracking error noted by *e(t)* and it is successive derivatives are defined as in (4) which is the main objective of the controller that minimizes this error to ensure accurate tracking. The sliding sector noted by *S(t)* and its three sub-surfaces (S_1, S_2, and S_3) are given in (5).

$$\begin{cases} e(t) = \omega_r - \omega_{r,opt} \\ \dot{e}(t) = \dot{\omega}_r - \dot{\omega}_{r,opt} \\ \ddot{e}(t) = \ddot{\omega}_r - \ddot{\omega}_{r,opt} \\ \dddot{e}(t) = f(e(t),t) + g(e(t),t) \times u(t) \end{cases} \tag{4}$$

where:

$$\begin{cases} f_1(e(t),t) = (a_{11}^3 + 2a_{13}a_{31}a_{11} + a_{13}a_{33}a_{31})\omega_r + (a_{13}a_{32}a_{22} + a_{13}a_{32}a_{11} + a_{13}a_{32}a_{33})\omega_g \\ f_2(e(t),t) = (a_{11}^2 a_{13} + a_{13}^2 a_{31} + a_{33}^2 a_{13} + a_{13}a_{32}a_{23} + a_{11}a_{13}a_{33})T_{ls} + (a_{13}a_{32}a_{24} + a_{11}a_{13}a_{34} + a_{13}a_{33}a_{34})T_{em} \\ f_3(e(t),t) = a_{13}a_{34}a_{45}I_{rq} + a_{13}a_{34}a_{46}I_{rd} + (a_{11}^2 c_{11} + a_{13}a_{31}c_{11} + a_{11}a_{13}c_{31} + a_{13}a_{33}c_{31})T_a \\ f_4(e(t),t) = (a_{11}c_{11} + a_{13}c_{31})\dot{T}_a + c_{11}\ddot{T}_a + a_{13}a_{34}c_{43}\emptyset_s - \dddot{\omega}_{r,opt} \\ f(e(t),t) = f_1(e(t),t) + f_2(e(t),t) + f_3(e(t),t) + f_4(e(t),t) \\ g(e(t),t) = a_{13}a_{34}b_4 \end{cases}$$

$$\begin{cases} S_1(t) = \ddot{e}(t) + G_1^1 \dot{e}(t) + G_0^1 e(t) \\ S_2(t) = \ddot{e}(t) + G_1^2 \dot{e}(t) + G_0^2 e(t) \\ S_3(t) = \ddot{e}(t) + G_1^3 \dot{e}(t) + G_0^3 e(t) \\ S(t) = \frac{S_1(t)+S_2(t)+S_3(t)}{3} = \ddot{e}(t) + G_1 \dot{e}(t) + G_0 e(t) \end{cases} \tag{5}$$

where, $G_1 = \frac{G_1^1 + G_1^2 + G_1^3}{3}$, and $G_0 = \frac{G_0^1 + G_0^2 + G_0^3}{3}$.

The control law consists of two terms the equivalent control term ($V_{rq,eq}$) and the switching control term ($V_{rq,d}$) which are expressed as in (6). Where the three regions R_1, R_2, and R_3 divide the entire state space. These regions are defined in (7). The stability is proven outside the sliding sector i.e., $e(t) \in R_1 \cup R_2$, and inside the sliding sector i.e., $e(t) \in R_3$ through the powerful Lyapunov function (LF) as in (8). This LF is positive and it is first-time derivative is negative.

$$\begin{cases} V_{rq,eq}(t) = -\frac{f(e(t),t)+G_1\ddot{e}(t)+G_0\dot{e}(t)}{g(e(t),t)} \\ V_{rq,d}(t) = \begin{cases} -\frac{\alpha}{g(e(t),t)}\sum_{i=1}^{3} sign(S_i) & if\ e(t) \in R_1 \cup R_2 \\ -\frac{\alpha}{g(e(t),t)}\frac{\sum_{i=1}^{3}S_i}{\sum_{i=1}^{3}|S_i|} & if\ e(t) \in R_3 \end{cases} \end{cases} \tag{6}$$

$$\begin{cases} R_1 = e(t)|\cap_{i=1}^2 S_i(t) > 0 \\ R_2 = e(t)|\cap_{i=1}^2 S_i(t) < 0 \\ R_3 = e(t)|\cup_{i,j=1}^2 S_i(t)S_j(t) \leq 0 \end{cases} \tag{7}$$

$$V(t) = \frac{1}{2}S^2(t) \tag{8}$$

3. SIMULATION RESULTS AND DISCUSSION

The developed nonlinear control law, which is called SSC law, is applied to the overall WT model. The modern WT consists of an aeroturbine connected to the DFIG. The principal characteristics of the WT used in this paper are mentioned in Table 2. The performance of the SSC control applied to the WT is investigated under a random and fast variable wind speed as depicted in Figure 2. The wind speed profile in Figure 2(a) presents the external perturbation of the WT over a duration of 40 seconds with its average wind speed is about 12 m/s.

Table 2. Wind energy conversion system characteristics

Characteristic	Value	Unit
Blade radius	21.65	m
Rotor external friction	27.36	N.m.rad^{-1}.s
Rotor inertia	325,000	Kg.m^2
Generator external friction	0.2	N.m.rad^{-1}.s
Generator inertia	34.4	Kg.m^2
Tip-speed ratio optimal	8.1484	Unitless
Slow shaft torsion	2,691,000	N.m.rad^{-1}
Rotor resistance	0.0061	Ω
Rotor inductance	0.0068	H
Stator inductance	0.0068	H
Mutual inductance	0.0067	H
Power coefficient optimal	0.4745	Unitless
Air density	1.29	Kg.m^{-3}
Slow shaft friction	9,500	N.m.rad^{-1}.s

The simulation results are performed using MATLAB toolboxes. The purpose of these simulation results is proving the effectiveness of the developed SSC technique by comparing it with the traditional SMC law under fast and unpredictable wind speed fluctuations. The two control laws (SMC and SSC) are tested for the same values of the switching gain during the same simulation time. The values of the control gains are indicated in Table 3.

Table 3. Control gains values

Gains	α	G_0^1	G_0^2	G_0^3	G_1^1	G_1^2	G_1^3
1st test of simulation	0.5	0.9	0.61	0.77	1.9	0.99	10.95
2nd test of simulation	3	0.9	0.61	0.77	1.9	0.99	10.95

Figure 2 depicts the wind speed curve and the temporal variation in rotor speed. Figure 2(b) illustrates the precise tracking of the rotor speed and its reference signal for both control laws SMC and SSC. From Figure 2(c), the value of the switching gain increases, and the rotor speed can quickly follow its reference signal. The good result shown in Figures 2(b) and 2(c) is the capability of achieving accurate tracking between the rotor speed and its desired signal. The precise tracking aims to extract the maximum power available whatever the climatic conditions of the wind.
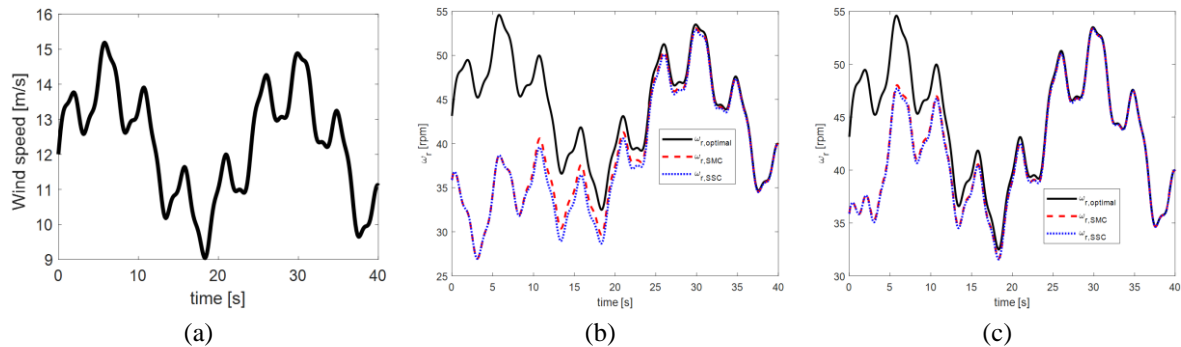

(a)   (b)   (c)

Figure 2. Wind speed fluctuations and WT rotor speed variation (a) wind speed profile, (b) 1st test of simulation, and (c) 2nd test of simulation

Figure 3 shows the temporal variation in generator torque. Figure 3(a) shows that both control laws SMC and SSC can maintain the generator torque within its limit. However, the chattering phenomenon appears in Figure 3(b) for the SMC law. The major inconvenience of the SMC is the chattering because it can lead to strong vibrations on the drive shafts of WT, and it affects the accuracy of the control system by introducing variability in the input variables. The same discussion of Figures 3(a) and 3(b) concerns Figures 3(c) and 3(d). When the value of the switching gain is increasing (here where the main contribution of SSC is represented), the chattering phenomenon becomes more important for the traditional SMC

technique. However, for the proposed control, the chattering phenomenon does not appear using a high value of switching gain.
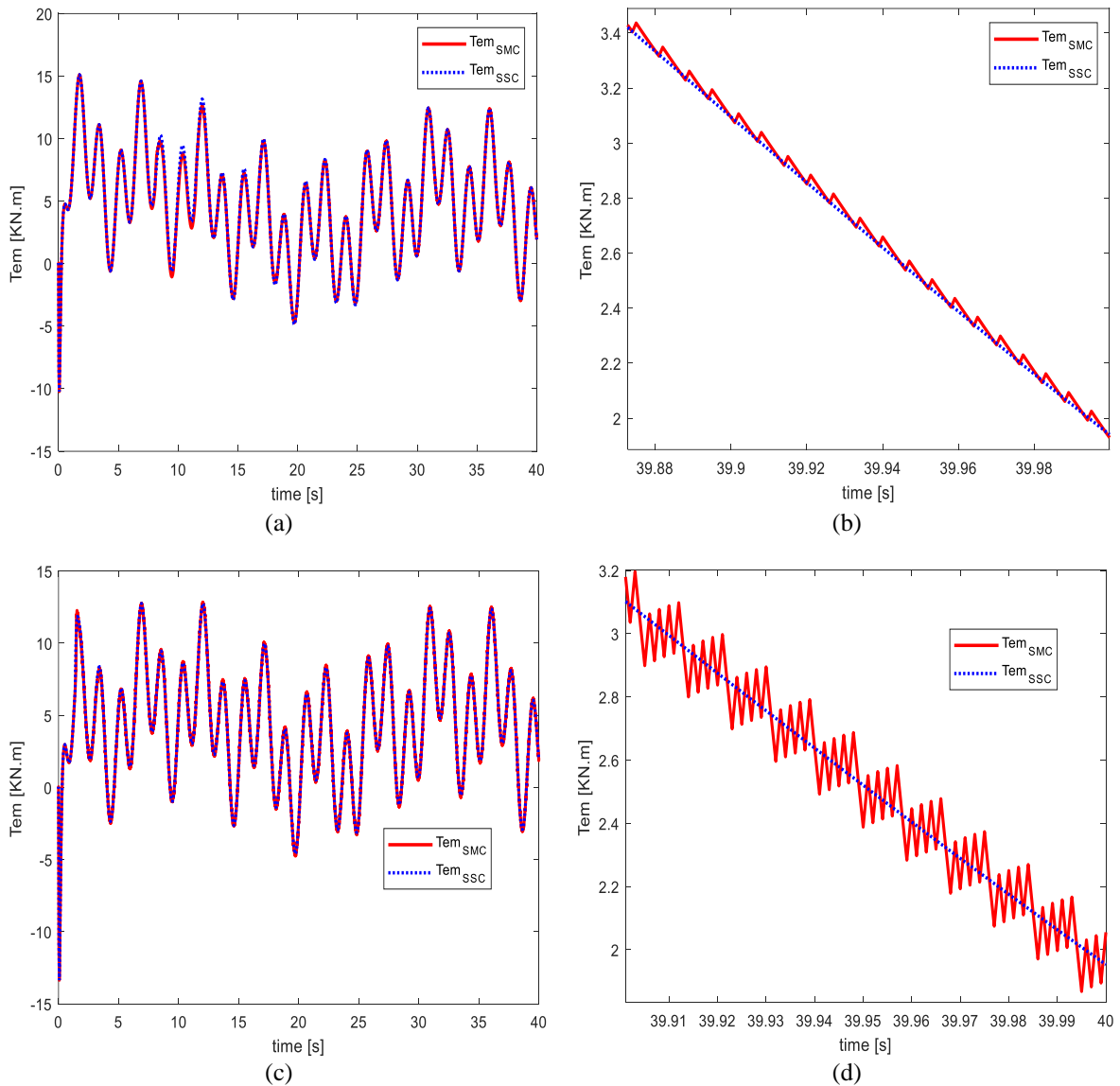

Figure 3. Generator torque variation (a) 1st test, (b) 1st test's Zome portion, (c) 2nd test, and (d) 2nd test's Zome portion

Figure 4(a) shows the DFIG rotor q-axis voltage to be imposed by the controller to reach the reference of the rotor speed. Therefore, the control strategy developed aims to obtain good performances by comparing it with the classical SMC when the chattering problem appears in the SMC as shown in Figure 4(b). The same discussion of Figures 4(a) and 4(b) concerns Figures 4(c) and 4(d). When the value of the switching gain is increasing (here the power of the SSC law appears), the chattering becomes more important for SMC. In contrast, the chattering problem does not appear by using a high value of switching gain for the developed control law.

To show clearly the effectiveness of the proposed control law in this paper, Figure 5 depicts the sliding surface of SMC, and the sliding sector of SSC strategy and its three sub-surfaces by using the high switching gain value. Figure 5(a) shows that the three sub-surfaces of the SSC technique converge gradually towards the sliding sector. Additionally, SSC law exhibits no oscillations that could lead to the chattering problem as illustrated in Figure 5(b).
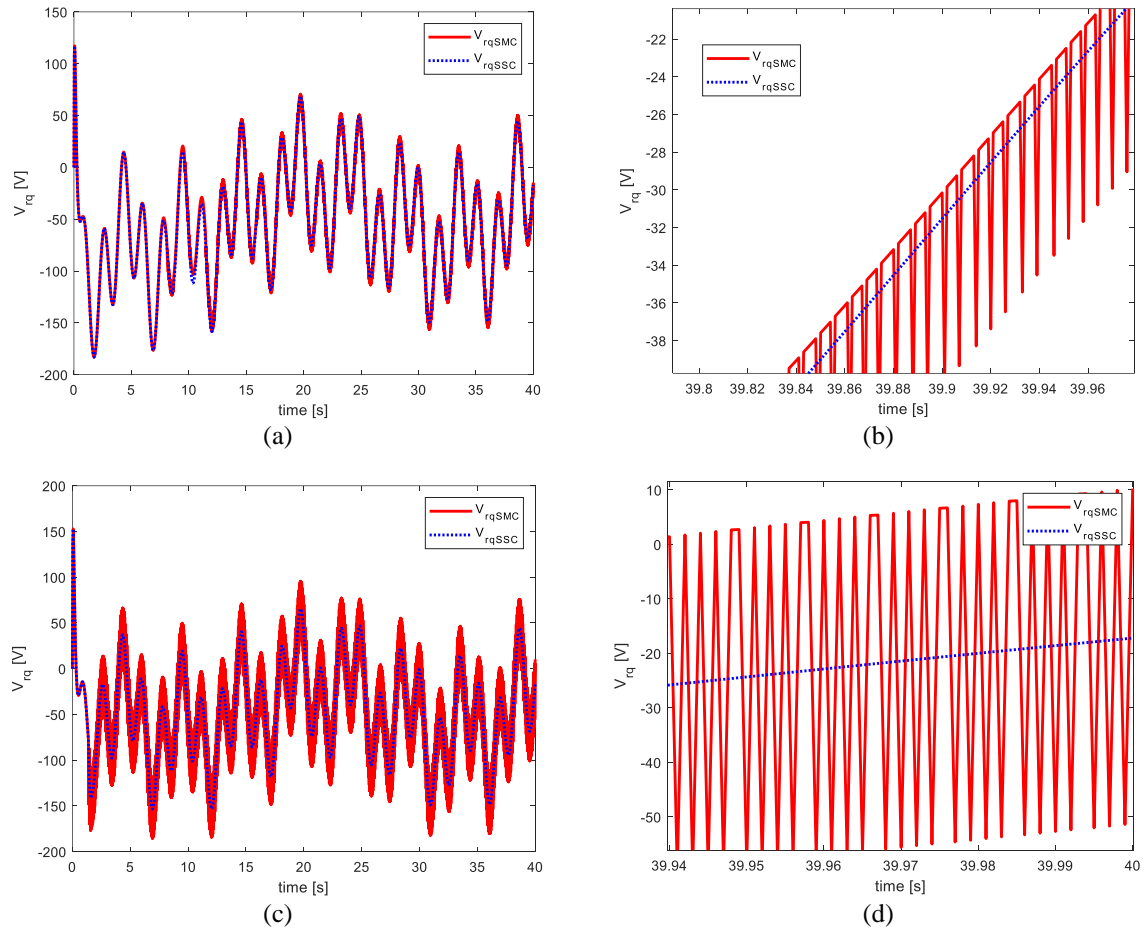
Figure 4. DFIG rotor q-axis voltage evolution (a) 1st test, (b) 1st test's Zome portion, (c) 2nd test, and (d) 2nd test's Zome portion
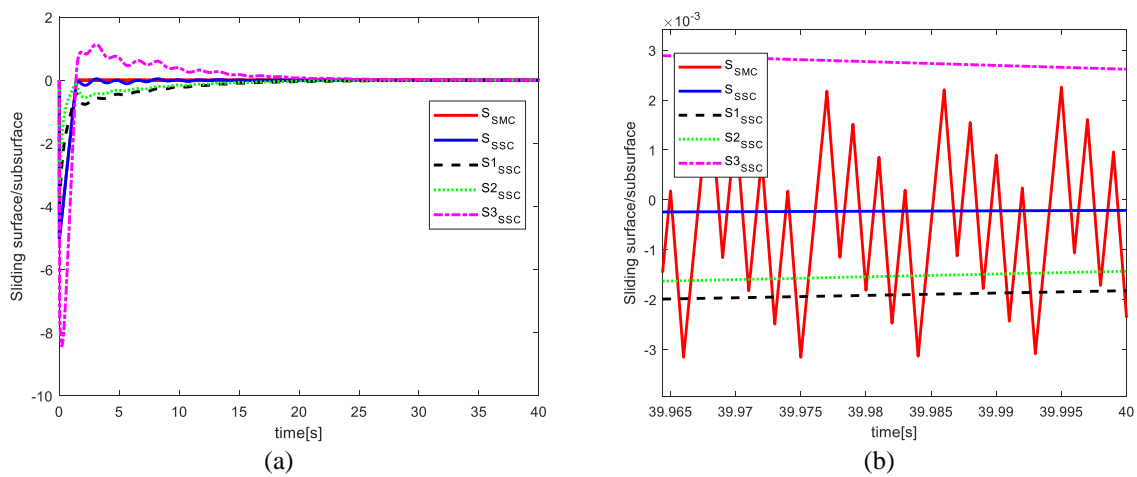

Figure 5. Sliding surface (a) time evolution of sliding surface and (b) zoom in portion of sliding surface

4. CONCLUSION

This paper presents a novel nonlinear control strategy for the entire wind energy conversion system operating under a variable speed wind by tacking it as a strong external disturbance. The proposed control is improved by transforming the sliding surface of the known classical sliding mode control into a sliding sector with the main objective of optimizing the performance of the wind turbine by making it more profitable. The simulation results obtained by MATLAB toolboxes prove the effectiveness of the proposed nonlinear control

approach in terms of obtaining the maximum wind power available whatever the climatic conditions associated with the wind, achieving a precise tracking of the optimal value of the rotor speed, reducing the aerodynamic loads of the turbine devices, eliminating the chattering phenomenon, and easy implementation in real-time.

REFERENCES

[1]　S. Toledo, M. Rivera, and J. L. Elizondo, "Overview of wind energy conversion systems development, technologies and power electronics research trends," in *2016 IEEE International Conference on Automatica (ICA-ACCA)*, Oct. 2016, pp. 1–6, doi: 10.1109/ICA-ACCA.2016.7778454.

[2]　Y.-D. Song, P. Li, W. Liu, and M. Qin, "An overview of renewable wind energy conversion system modeling and control," *Measurement and Control*, vol. 43, no. 7, pp. 203–208, Sep. 2010, doi: 10.1177/002029401004300703.

[3]　M. Balat, "A review of modern wind turbine technology," *Energy Sources, Part A: Recovery, Utilization, and Environmental Effects*, vol. 31, no. 17, pp. 1561–1572, Oct. 2009, doi: 10.1080/15567030802094045.

[4]　M. A. Ahmad, J. J. Jui, and M. R. Ghazali, "Using adaptive safe experimentation dynamics algorithm for maximizing wind farm power production," in *2022 57th International Universities Power Engineering Conference (UPEC)*, Aug. 2022, pp. 1–4, doi: 10.1109/UPEC55022.2022.9917785.

[5]　W. Song *et al.*, "A novel wind turbine control strategy to maximize load capacity in severe wind conditions," *Energy Reports*, vol. 8, pp. 7773–7779, Nov. 2022, doi: 10.1016/j.egyr.2022.06.005.

[6]　A. Mohammadi, S. Farajianpour, S. Tavakoli, and S. M. Barakati, "Fluctuations mitigation of variable speed wind turbine through optimized centralized controller," *TELKOMNIKA (Telecommunication Computing Electronics and Control)*, vol. 10, no. 4, pp. 703–714, Dec. 2012, doi: 10.12928/telkomnika.v10i4.859.

[7]　M. Gustavo and P. Enrique, "Modelling and control design of pitch-controlled variable speed wind turbines," in *Wind Turbines*, InTech, 2011.

[8]　A. Mishra, P. M. Tripathi, and K. Chatterjee, "A review of harmonic elimination techniques in grid connected doubly fed induction generator based wind energy system," *Renewable and Sustainable Energy Reviews*, vol. 89, pp. 1–15, Jun. 2018, doi: 10.1016/j.rser.2018.02.039.

[9]　M. Sadek, M. Elkholy, and H. Metwally, "Efficient operation of wind turbine with doubly fed induction generator using TLBO algorithm and artificial neural networks," *International Review on Modelling and Simulations (IREMOS)*, vol. 9, no. 6, Dec. 2016, doi: 10.15866/iremos.v9i6.10309.

[10]　F. M. Ebrahimi, A. Khayatiyan, and E. Farjah, "A novel optimizing power control strategy for centralized wind farm control system," *Renewable Energy*, vol. 86, pp. 399–408, Feb. 2016, doi: 10.1016/j.renene.2015.07.101.

[11]　H. J. Asl and J. Yoon, "Power capture optimization of variable-speed wind turbines using an output feedback controller," *Renewable Energy*, vol. 86, pp. 517–525, Feb. 2016, doi: 10.1016/j.renene.2015.08.040.

[12]　M. Rahimi, "Coordinated control of rotor and grid sides converters in DFIG based wind turbines for providing optimal reactive power support and voltage regulation," *Sustainable Energy Technologies and Assessments*, vol. 20, pp. 47–57, Apr. 2017, doi: 10.1016/j.seta.2017.02.012.

[13]　P. K. Gayen, D. Chatterjee, and S. K. Goswami, "Stator side active and reactive power control with improved rotor position and speed estimator of a grid connected DFIG (doubly-fed induction generator)," *Energy*, vol. 89, pp. 461–472, Sep. 2015, doi: 10.1016/j.energy.2015.05.111.

[14]　B. Rached, M. Elharoussi, and E. Abdelmounim, "Design and investigations of MPPT strategies for a wind energy conversion system based on doubly fed induction generator," *International Journal of Electrical and Computer Engineering (IJECE)*, vol. 10, no. 5, pp. 4770–4781, Oct. 2020, doi: 10.11591/ijece.v10i5.pp4770-4781.

[15]　J. Zhang, Y. Wan, Q. Ouyang, and M. Dong, "Nonlinear stochastic adaptive control for DFIG-based wind generation system," *Energies*, vol. 16, no. 15, Jul. 2023, doi: 10.3390/en16155654.

[16]　I. Munteanu, N. A. Cutululis, A. I. Bratcu, and E. Ceangă, "Optimization of variable speed wind power systems based on a LQG approach," *Control Engineering Practice*, vol. 13, no. 7, pp. 903–912, Jul. 2005, doi: 10.1016/j.conengprac.2004.10.013.

[17]　F. Wu, X.-P. Zhang, K. Godfrey, and P. Ju, "Small signal stability analysis and optimal control of a wind turbine with doubly fed induction generator," *IET Generation, Transmission and Distribution*, vol. 1, no. 5, 2007, doi: 10.1049/iet-gtd:20060395.

[18]　N. Hamadi, H. Imine, D. Ameddah, and A. Chari, "Tires-road forces estimation: Using sliding mode and triangular observer," *IFAC Journal of Systems and Control*, vol. 7, Mar. 2019, doi: 10.1016/j.ifacsc.2019.100032.

[19]　R. Santos and T. R. Oliveira, "Trajectory tracking for uncertain (non) minimum phase systems by monitoring function and time-scaling based sliding mode control," *IFAC Journal of Systems and Control*, vol. 12, Jun. 2020, doi: 10.1016/j.ifacsc.2020.100089.

[20]　Y. Berrada, E. Boufounas, and I. Boumhidi, "Optimal neural network sliding mode control without reaching phase using genetic algorithm for a wind turbine," in *2015 10th International Conference on Intelligent Systems: Theories and Applications (SITA)*, Oct. 2015, pp. 1–6, doi: 10.1109/SITA.2015.7358405.

[21]　J. Mérida, L. T. Aguilar, and J. Dávila, "Analysis and synthesis of sliding mode control for large scale variable speed wind turbine for power optimization," *Renewable Energy*, vol. 71, pp. 715–728, Nov. 2014, doi: 10.1016/j.renene.2014.06.030.

[22]　B. Beltran, T. Ahmed-Ali, and M. E. H. Benbouzid, "Sliding mode power control of variable-speed wind energy conversion systems," *IEEE Transactions on Energy Conversion*, vol. 23, no. 2, pp. 551–558, Jun. 2008, doi: 10.1109/TEC.2007.914163.

[23]　V. Utkin and H. Lee, "Chattering problem in sliding mode control systems," *IFAC Proceedings Volumes*, vol. 39, no. 5, 2006, doi: 10.3182/20060607-3-IT-3902.00003.

[24]　Y. Berrada and I. Boumhidi, "New structure of sliding mode control for variable speed wind turbine," *IFAC Journal of Systems and Control*, vol. 14, Dec. 2020, doi: 10.1016/j.ifacsc.2020.100113.

[25]　Z. Lahlou, Y. Berrada, and I. Boumhidi, "Nonlinear feedback control for a complete wind energy conversion system," *International Review of Automatic Control (IREACO)*, vol. 12, no. 3, May 2019, doi: 10.15866/ireaco.v12i3.16656.

[26]　J. T. Jose and A. B. Chattopadhyay, "Modeling of the magnetizing phenomena of doubly fed induction generator using neuro-fuzzy algorithm considering non-linearity," *International Journal of Electrical and Computer Engineering (IJECE)*, vol. 9, no. 1, pp. 23–33, Feb. 2019, doi: 10.11591/ijece.v9i1.pp23-33.

[27]　H. Hachemi, A. Allali, and B. Belkacem, "Control of the powerquality for a DFIG powered by multilevel inverters," *International Journal of Electrical and Computer Engineering (IJECE)*, vol. 10, no. 5, pp. 4592–4603, Oct. 2020, doi: 10.11591/ijece.v10i5.pp4592-4603.

BIOGRAPHIES OF AUTHORS

Yattou El Fadili [iD] [image] [SC] [image] received B.Sc. in physics 'Electronic Option' in 2019, and obtained M.Sc. in microelectronics, signals, and systems in 2021 from the Faculty of Sciences Dhar El Mahraz, Sidi Mohamed Ben Abdellah University of Fez in Morocco. She is currently a Ph.D. student at the Computer Science, Signal, Automation, and Cognitivism Laboratory at the Faculty of Sciences in Fez-Morocco. Her current research interests include modeling and control of wind turbine energy conversion systems. She can be contacted at email: yattou.elfadili@usmba.ac.ma.

Youssef Berrada [iD] [image] [SC] [image] received Ph.D. degree from the Laboratory of Electronics, Signals, Systems and Informatics, Physics Department, Faculty of Sciences Sidi Mohamed Ben Abdellah University in 2018, M.Sc. in Signals, Systems and Computer from the Faculty of Sciences, Fez Morocco in 2013, and B.Sc. in Mechanical, Automation, and Electro-Mechanics from Polydisciplinary Faculty Taza, Morocco in 2011. His research interests include modeling, control, and optimization of wind turbine energy conversion systems. He can be contacted at email: youssef.berrada@usmba.ac.ma.

Ismail Boumhidi [iD] [image] [SC] [image] is a professor of electronic and automatic at the Faculty of Sciences, Fez Morocco, received Ph.D. degree from Sidi Mohamed Ben Abdellah University, Faculty of Sciences in 1994 and a state Ph.D. degree in 1999. His research areas include adaptive and robust control, multivariable nonlinear systems, fuzzy logic control with applications, and renewable energies. He can be contacted at email: ismail.boumhidi@usmba.ac.ma.